REPRODUCTION
RESEARCH

Spermatid development in XO male mice with varying Y chromosome short-arm gene content: evidence for a Y gene controlling the initiation of sperm morphogenesis

Nadège Vernet, Shantha K Mahadevaiah, Peter J I Ellis[1], Dirk G de Rooij[2] and Paul S Burgoyne

Division of Stem Cell Biology and Developmental Genetics, MRC National Institute for Medical Research, The Ridgeway, Mill Hill, London NW7 1AA, UK, [1]Mammalian Molecular Genetics Group, Department of Pathology, University of Cambridge, Cambridge CB2 1QP, UK and [2]Center for Reproductive Medicine, Amsterdam Medical Center, University of Amsterdam, 1105 AZ Amsterdam, The Netherlands

Correspondence should be addressed to N Vernet; Email: vernet.nadege@gmail.com

Abstract

We recently used three XO male mouse models with varying Y short-arm (Yp) gene complements, analysed at 30 days *post partum*, to demonstrate a Yp gene requirement for the apoptotic elimination of spermatocytes with a univalent X chromosome at the first meiotic metaphase. The three mouse models were i) X*Sxr*^{a}O in which the Yp-derived Tp(Y)1Ct$^{Sxr\text{-}a}$ sex reversal factor provides an almost complete Yp gene complement, ii) X*Sxr*^{b}O,*Eif2s3y* males in which Tp(Y)1Ct$^{Sxr\text{-}b}$ has a deletion completely or partially removing eight Yp genes – the Yp gene *Eif2s3y* has been added as a transgene to support spermatogonial proliferation, and iii) XO*Sry*,*Eif2s3y* males in which the *Sry* transgene directs gonad development along the male pathway. In this study, we have used the same mouse models analysed at 6 weeks of age to investigate potential Yp gene involvement in spermiogenesis. We found that all three mouse models produce haploid and diploid spermatids and that the diploid spermatids showed frequent duplication of the developing acrosomal cap during the early stages. However, only in X*Sxr*^{a}O males did spermiogenesis continue to completion. Most strikingly, in XO*Sry*,*Eif2s3y* males, spermatid development arrested at round spermatid step 7 so that no sperm head restructuring or tail development was observed. In contrast, in X*Sxr*^{b}O,*Eif2s3y* males, spermatids with substantial sperm head and tail morphogenesis could be easily found, although this was delayed compared with X*Sxr*^{a}O. We conclude that *Sxr*^{a} (and therefore Yp) includes genetic information essential for sperm morphogenesis and that this is partially retained in *Sxr*^{b}.

Reproduction (2012) **144** 433–445

Introduction

Spermatogenesis consists of three distinct phases: the proliferative phase, in which spermatogonia undergo successive mitotic divisions to assure both germ cell production and maintenance of the tissue by stem cell renewal, the meiotic phase in which spermatocytes undergo two consecutive divisions to produce haploid spermatids and the spermiogenesis phase in which haploid round spermatids differentiate into sperm. During the spermiogenesis phase, there is extensive nuclear restructuring involving the replacement of histones by protamines in conjunction with elongation and condensation of the nucleus to form the sperm head. Meanwhile, the spermatids develop an acrosome that is a cap-like structure containing the enzymes necessary to break down the outer membrane of the egg during fertilization, and a tail (flagellum) is formed.

It has long been known that spermiogenesis can occur in the absence of the second meiotic division, thus generating spermatids with a 2C DNA content 'diploid spermatids' (Hannappel & Drews 1979, Hannappel *et al.* 1980, Levy & Burgoyne 1986, Kot & Handel 1990, Mori *et al.* 1999). For instance, in X*Sxr*^{a}O male mice where the X chromosome carries the Y chromosome short-arm (Yp)-derived Tp(Y)1Ct$^{Sxr\text{-}a}$ 'sex reversal' factor (Fig. 1), a massive apoptotic elimination occurs at the metaphase of the first meiotic division (MI) in response to the sex chromosome univalence (Levy & Burgoyne 1986, Kot & Handel 1990, Sutcliffe *et al.* 1991). However, a very small proportion of MI spermatocytes do not apoptose; the majority of these do not undergo the second meiotic division and remain diploid, while a minority do complete the second meiotic division to become haploid (Levy & Burgoyne 1986, Sutcliffe *et al.* 1991). Subsequently, the diploid and haploid cells initiate the

DOI: 10.1530/REP-12-0158
ISSN 1470–1626 (paper) 1741–7899 (online)
Online version via www.reproduction-online.org

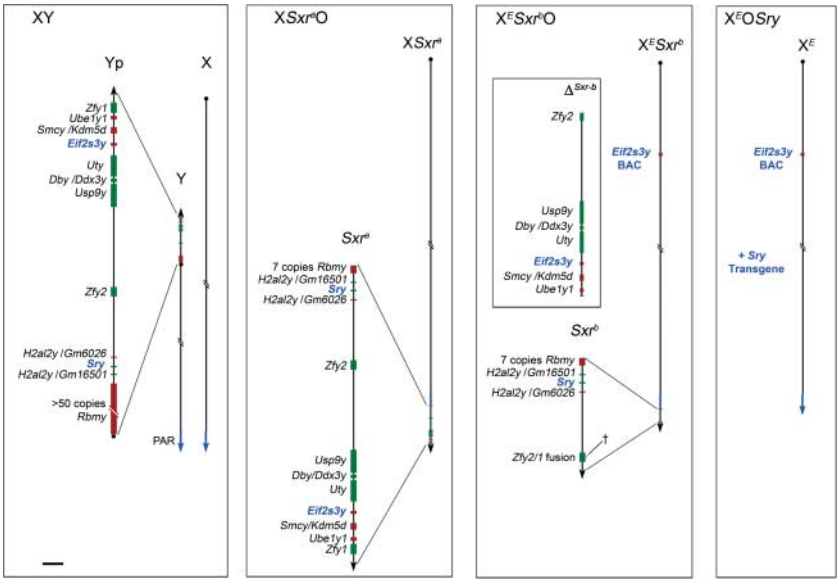

Figure 1 Schematic diagrams showing the Y gene complements of XO male mice. The mouse Y short-arm (Yp; represented to scale in the magnified view) has seven single copy genes, two duplicated genes and one multi copy gene (*Gm6026* and *Gm16501* encode a novel histone of the H2A superfamily; hereafter named *H2al2y*). Transcriptional senses are shown in red for the forward strands and in green for the reverse strands. (Note that the mouse Y has a single distal pseudoautosomal region (PAR) on the long arm). In X*Sxr*^{a}O males, the Y chromosome short-arm derived *Sxr*^{a} sex reversal factor, here attached distal to the PAR on the X chromosome includes most of the Yp genes. In X^E*Sxr*^{b}O males, the *Sxr*^{a}-derived deletion variant *Sxr*^{b} has a 1.3 Mb deletion (Δ^{Sxrb}) removing six single-copy genes and creating a *Zfy2/1* fusion gene spanning the deletion break point (†). The X-linked *Eif2s3y* Y genomic BAC transgene (Mazeyrat *et al.* 2001) is represented on the X chromosome but its site of integration was not assessed. X^{E}O*Sry* males lack Y chromosome but have the minimum Y gene complement compatible with progression to the first meiotic metaphase: the X-located *Eif2s3y* BAC transgene and an autosomally located *Sry* transgene. The Y genes common to all three XO male models (i.e. *Sry* and *Eif2s3y*) are represented in blue. Scale bar for magnified views is 150 kb.

condensation phase of spermiogenesis and there is substantial head morphogenesis – albeit abnormal due to the absence of the Y long-arm (Burgoyne *et al.* 1992, Cocquet *et al.* 2009). The occurrence of spermiogenesis in the absence of the second meiotic division is not unique to mice with an abnormal sex chromosome complement, as it is also seen in male T(6;12)32H carriers where a reciprocal translocation between autosomes 6 and 12 results in incomplete chromosome pairing and diploid spermatids are generated (de Boer *et al.* 1986).

Recently, we investigated the DNA content of the meiotic products in two XO male mouse models with a deficient Yp gene complement (Vernet *et al.* 2011). In the first model, the Y gene complement is provided by transgenic copies of *Sry* (on an autosome) and *Eif2s3y* (on the X chromosome) and in the second *Sry* is replaced by Tp(Y)1Ct$^{Sxr\text{-}b}$, a derivative of *Sxr*^{a} with a deletion removing most Yp genes but retaining *Sry*. These models are here denoted as X^{E}O*Sry* and X^E*Sxr*^{b}O respectively (Fig. 1). At 30 dpp in both models, meiosis was found to be blocked in the interphase between the first and the second meiotic division so that no haploid spermatids were produced. In control males at this age, both meiotic divisions are completed and elongating spermatids are already seen (Vernet *et al.* 2011). In the X^{E}O*Sry* males, we further showed that during epithelial stages II–III, the interphasic secondary spermatocytes with 2C DNA lost the SYCP3 staining typical of interphasic secondary spermatocytes; in wild-type mice, SYCP3 is lost at the same epithelial stage following the secondary spermatocyte to haploid round spermatid transition (Vernet *et al.* 2011). This observation therefore suggested that diploid interphasic secondary spermatocytes also enter spermiogenesis to become diploid round spermatids. However, no progression to elongating spermatid stages was seen at 30 dpp. In a separate study, Decarpentrie *et al.* (2012) reported that in X^E*Sxr*^{b}O testis from 30 dpp onwards, expression from the *Zfy2* spermatid-specific *Cypt*-derived promoter was detected, which again suggests entry into spermiogenesis. Finally, Mazeyrat *et al.* (2001) claimed that there were some elongating spermatid stages in these two Yp gene-deficient models when analysed at substantially older ages.

These previous studies suggested that spermiogenesis was initiated in these Yp-deficient models, so we therefore sought to determine the extent of spermiogenic progression in X^{E}O*Sry* and X^E*Sxr*^{b}O males in comparison to that seen in X*Sxr*^{a}O mice, which have an almost complete Yp gene complement.

Results

Completion of the second meiotic division in X^{E}OSry and X^{E}Sxr^{b}O mice at 6 weeks of age

In our published study (Vernet *et al.* 2011), the DNA content of post-meiotic cells was assessed at 30 dpp.

This age was chosen because the DNA analysis was linked to a study of MI spermatocyte apoptosis, and at later ages, apoptotic interphasic secondary spermatocytes from the previous cycle interfered with the quantitation of MI spermatocyte apoptosis. For the current study of spermiogenic progression, we wished to analyse 6-week-old males when spermatogenesis is fully established, but when there is none of the secondary damage resulting in disturbed spermatogenesis and spermatogonial and spermatocyte loss that is seen in older males (Mazeyrat *et al*. 2001).

The appropriate XO control males for this study are X*Sxr*^{a}O, which have an almost complete Yp gene complement. For comparison with previous data from 30 dpp X^{E}O*Sry* and X^E*Sxr*^{b}O males (Vernet *et al*. 2011), we first quantified the DNA content in spread spermatogenic cells from three 30 dpp X*Sxr*^{a}O males. In contrast to the lack of haploid spermatids in the Yp-deficient mouse models, haploid round spermatids were identified in two of the three X*Sxr*^{a}O males analysed with an average of 8.7% of spermatids being haploid (Table 1). At 6 weeks, all four X*Sxr*^{a}O males analysed had a greater proportion of haploid spermatids with an average of 44.1%. These results indicate that in X*Sxr*^{a}O males the, second meiotic division occurs more often after the first spermatogenic wave.

Analysis of the DNA content of post-meiotic cells in four 6-week-old X^{E}O*Sry* and X^E*Sxr*^{b}O mice showed a low frequency of haploid spermatids in both genotypes varying from 1.5 to 18.4% (Table 1). This indicates that the block at the interphase stage of secondary spermatocytes observed at 30 dpp has become leaky by 6 weeks of age. However, the proportion of haploid spermatids obtained is significantly less than in age-matched X*Sxr*^{a}O males.

Acrosomal development is seen in spermatids of X^{E}OSry and X^{E}Sxr^{b}O males but substantial head elongation is restricted to X^{E}Sxr^{b}O males

The development of the acrosome in mouse spermatids is divided into four phases, Golgi (steps 1–3), cap (steps 4–6), acrosomal (steps 7–9) and maturation phases (steps 10–16), based on light microscopic analysis of periodic acid-Schiff (PAS)-stained testis sections and transmission electron microscopy (TEM; Oakberg 1956*b*, Russell *et al*. 1990). During the Golgi phase, numerous pro-acrosomic granules are formed within Golgi vesicles followed by a clustering into a vesicle containing a single acrosomic granule that associates with the nuclear envelope. During the subsequent cap and acrosomal phases, the acrosome increases in size by fusion of additional Golgi-derived vesicles and spreads over the anterior nuclear pole. The acrosome covers two thirds of the nucleus at the end of the acrosomal phase and achieves its definitive hook shape during the maturation phase.

Although X*Sxr*^{a}O mice produce very few, predominantly diploid, round spermatids, these nevertheless proceed through spermiogenesis; however, the sperm formed are grossly abnormal (Levy & Burgoyne 1986, Kot & Handel 1990, Sutcliffe *et al*. 1991). This spermiogenic progression is reflected in acrosomal changes that become apparent in PAS-stained (Supplementary Figure 1, see section on supplementary data given at the end of this article) and peanut agglutinin lectin (Lectin–PNA)-stained sections (Fig. 2) of 6-week-old males. As in XY controls, the few round spermatids of X*Sxr*^{a}O males progressively developed an acrosomal structure. However, while a single acrosomal structure was found at the nucleus of wild-type spermatids, in X*Sxr*^{a}O round spermatids, double and sometime multiple acrosomal structures were often detected (see stages IV–VI from Fig. 2). In order to assess whether this aberrant acrosome development was a consequence of diploidy, we recorded the incidence of aberrant acrosomes in haploid and diploid spermatids in sections stained with Lectin–PNA and 4′,6-diamidino-2-phenylindole (DAPI), using the contralateral testes from the two X*Sxr*^{a}O males with the higher percentage of haploid spermatids from the testis cell spread analysis. Diploid round spermatids can be confidently identified in the DAPI-stained sections because multiple nucleolus-like structures are observed and the nuclei are a third larger in diameter than those of haploid round spermatids. In stage IV–V tubules, we found a very significant ($P<0.00001$) preponderance of multiple acrosome structures (chromocentra) in diploid spermatids, although some were present in haploid round spermatids (Table 2). We therefore assessed the frequency of multiple acrosome structures in stages IV–V tubules in XY males, and this revealed a similar frequency to that obtained for the haploid round spermatids from the X*Sxr*^{a}O males. Elongation of the sperm head becomes apparent from stage IX onwards, and by this stage, the acrosome anomalies were no longer apparent for X*Sxr*^{a}O males (see stages IX–I from Fig. 2). The lack of acrosome anomalies during this acrosomic phase suggests either a fusion of the multiple acrosomal structures or selective loss of the spermatids with aberrant acrosomes.

Table 1 Haploid spermatid production in 30 dpp and 6-week-old XY and XO male mice. Data collected after DNA quantitation using DAPI fluorescence intensity measurement on SYCP3-labelled testis cell spreads. Values are mean ± S.E.M.

Genotype	Age (dpp)	Haploid (%)	Values range
XY ($n=3$)	30	98.2 ± 0.9*	96.8–100
X*Sxr*^{a}O ($n=3$)	30	8.7 ± 4.4	0–15.2
XY ($n=3$)	40–45	99.1 ± 0.8*	97.2–100
X*Sxr*^{a}O ($n=4$)	42–45	44.1 ± 7.3	21.3–52.6
X^{E}O*Sry* ($n=4$)	41–45	11.4 ± 3.1*	5.4–18.4
X^E*Sxr*^{b}O ($n=4$)	42–45	5.2 ± 1.2*	1.5–6.9

*Very significantly different from age-matched X*Sxr*^{a}O ($P\leq0.001$; ANOVA).

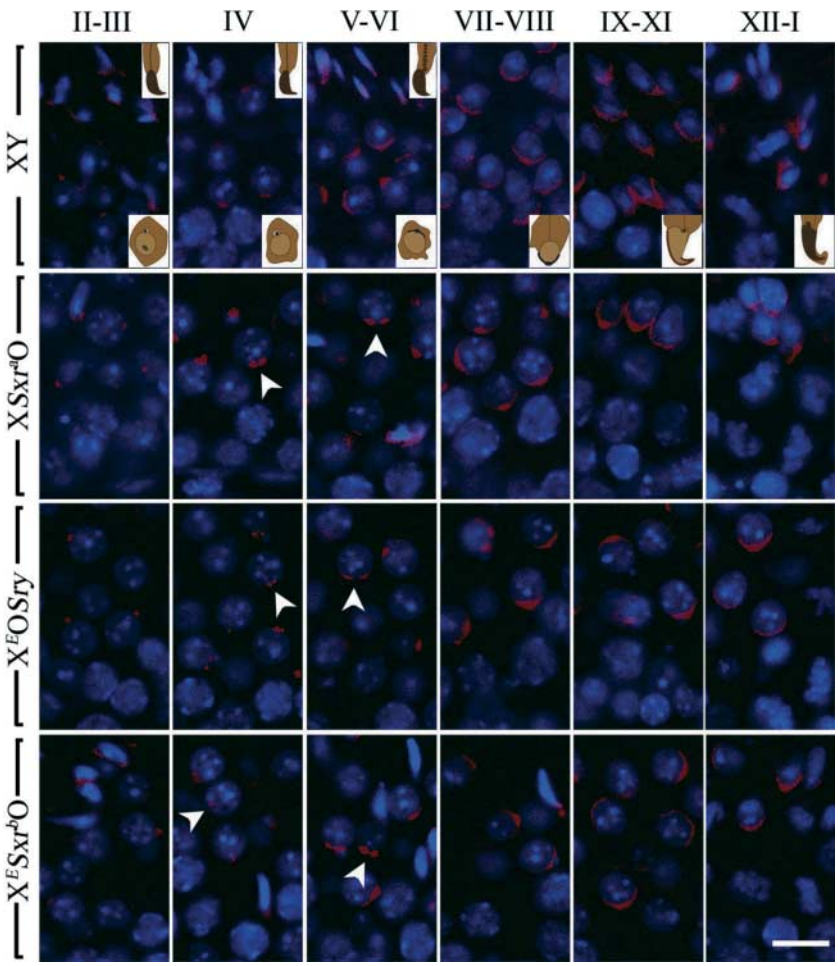

Figure 2 An acrosome is formed in all three genotypes of XO male mice. Acrosomes were detected with Lectin–PNA (red) on testis sections from 6-week-old XY, X*Sxr*^{a}O, X^{E}O*Sry* and X^E*Sxr*^{b}O mice. DAPI (blue) was used as a nuclear stain. Stages of seminiferous tubules are indicated and schematic diagrams of the spermatids appearing at each stage are represented for the XY control. Acrosome development in post-MI germ cells of X*Sxr*^{a}O, X^{E}O*Sry* and X^E*Sxr*^{b}O mice is synchronous with the acrosome development in XY round spermatids. However, double acrosomal structures (arrowheads) are observed in spermatids from X*Sxr*^{a}O, X^{E}O*Sry* and X^E*Sxr*^{b}O males from stage IV to stage VI. Elongated spermatids are found in XY and X*Sxr*^{a}O seminiferous tubules from stage IX onwards and in X^E*Sxr*^{b}O from stage XII onwards. Scale bar, 15 μm.

As in X*Sxr*^{a}O males, acrosome development in X^{E}O*Sry* and X^E*Sxr*^{b}O males appeared synchronous with controls, but once again, there were frequent double or multiple acrosomal structures that were no longer apparent by the acrosomal phase (Fig. 2; Supplementary Figure 1). As in X*Sxr*^{a}O males, diploid round spermatids from X^{E}O*Sry* and X^{E}S*xr*^{b}O testis show multiple DAPI bright chromocentra while haploid round spermatids contain one chromocentrum. The defects in acrosome formation in X^{E}O*Sry* males were confirmed by TEM analysis (Fig. 3). Thus, in XY control mice, the acrosome of step 3–8 round spermatids develops as a single structure at one side of the nucleus, while in X^{E}O*Sry* males two or more acrosomal structures were often found at the spermatid nucleus at the beginning of the cap phases (Fig. 3A, B, C and D). We occasionally found a discontinuous acrosomal structure at the nucleus of step 6 spermatids, but by the end of the cap phase, no obvious acrosome anomalies were observed (Fig. 3F, G and H).

Despite the comparable acrosome development, it was apparent from the PAS- and Lectin–PNA-stained sections that sperm head morphogenesis in stage IX tubules and beyond was not comparable to that in the X*Sxr*^{a}O controls. This was most obvious in X^{E}O*Sry* testes where we could see no clear evidence of the elongation or condensation of the spermatid nuclei that marks the development of the sperm head (Fig. 2, stages XII-I through IV). As it has previously been suggested that sperm head elongation can be seen to some extent in X^{E}O*Sry* testes (Mazeyrat *et al.* 2001), we did further analysis of haematoxylin and eosin (H&E)- and PAS-stained sections but again we did not find any clear evidence of elongation. Indeed, close examination of the PAS-stained material suggested that X^{E}O*Sry* spermatids almost never re-orientate to bring the acrosome to face the basal membrane, which in X*Sxr*^{a}O and XY controls marks the progression from steps 7 to 8 of round spermatid development, just before elongation (Fig. 4A). As the acrosome was fully formed around the spermatid nucleus, it is clear that step 7 round spermatids are typically the most advanced germ cells in X^{E}O*Sry* testes. Interestingly, the round spermatids arrested in step 7 do not enter apoptosis directly as these cells were observed until stage V of the next cycle. However, in stages XI–IV, remnants of dying round

Table 2 The frequency of double/multiple acrosomal structures in haploid or diploid spermatids of stages IV–V tubules for 6-week-old X*Sxr*^{a}O and XY male mice.

Mouse ID	Percentage of haploid spermatids[a] (*n*=number of cells analysed)	Percentage of cells with double or multiple acrosomal structures		
		Haploid	Diploid	χ^2; *P* value[b]
X*Sxr*^{a}O #1	38.7 (*n*=111)	9.3	52.9	21.8; *P*=0.000003
X*Sxr*^{a}O #2	46.6 (*n*=131)	16.4	62.9	29.0; *P*=0.00000007
XY #1	100 (*n*=253)	10.2	–	–
XY #2	100 (*n*=249)	13.1	–	–

[a]See Table 1 for the percentages of haploid spermatids estimated from cell spreads from the contralateral testes. [b]χ^2 analysis comparing the frequency of double/multiple acrosomal structures in diploid vs haploid spermatids in X*Sxr*^{a}O males.

spermatids and some rare possibly elongating spermatids with a darkly stained nucleus (classically associated with apoptosis/necrosis) were present that could have been confused previously with elongated spermatid nuclei (Mazeyrat *et al*. 2001), indicating that the arrested step 7 spermatids slowly disappeared by apoptosis/necrosis (Fig. 4B; Supplementary Figure 1). However, we have also seen apparently healthy round spermatids in the epididymis (data not shown), indicating that the arrested cells can also be shed from the epithelium.

In contrast to X^{E}O*Sry*, in 6-week-old X^E*Sxr*^{b}O males, nuclear elongation was evident (Fig. 4) as previously reported for older males (Mazeyrat *et al*. 2001). This difference in the stage of development reached is consistent with the fact that at 6 weeks of age, X^E*Sxr*^{b}O testes were significantly larger than those from X^{E}O*Sry* (57.8±0.28 mg X^E*Sxr*^{b}O and 49.8±0.33 mg X^{E}O*Sry*; *P*=0.0218). However, relative to X*Sxr*^{a}O and XY controls, sperm head elongation was delayed from stage IX to stage XII-I and nuclear condensation was delayed from stage XII until stages II–III (Figs 2 and 4).

Spermatid elongation in X^{E}Sxr^{b}O in relation to ploidy

The 'leak' in the sperm head elongation arrest at 61 dpp in X^E*Sxr*^{b}O mice is more extensive at 98 dpp with multiple clumps of elongating spermatids observed in the seminiferous tubules (Mazeyrat *et al*. 2001). In this study, in X^E*Sxr*^{b}O mice, we have also easily found tubules with elongating spermatids in 6-week-old testes, whereas at 30 dpp, elongating spermatids are absent; in X*Sxr*^{a}O testes, elongating spermatids are frequent at 30 dpp (Supplementary Figure 2, see section on supplementary data given at the end of this article). These age and genotype effects on the frequency of elongating spermatids mirrors the age and genotype effects on the frequency of haploid spermatids, suggesting that haploidy may promote sperm head elongation. To test this, we analysed the ploidy of round and elongating spermatids by quantification of DNA FISH signals in 6-week-old males (Fig. 5). This analysis not only confirmed the low frequency of haploid round spermatids in X^E*Sxr*^{b}O males (5% haploid and 95% diploid) but also revealed that haploid and diploid spermatids can elongate with equal efficiency (6% haploid and 94% diploid) (Table 3).

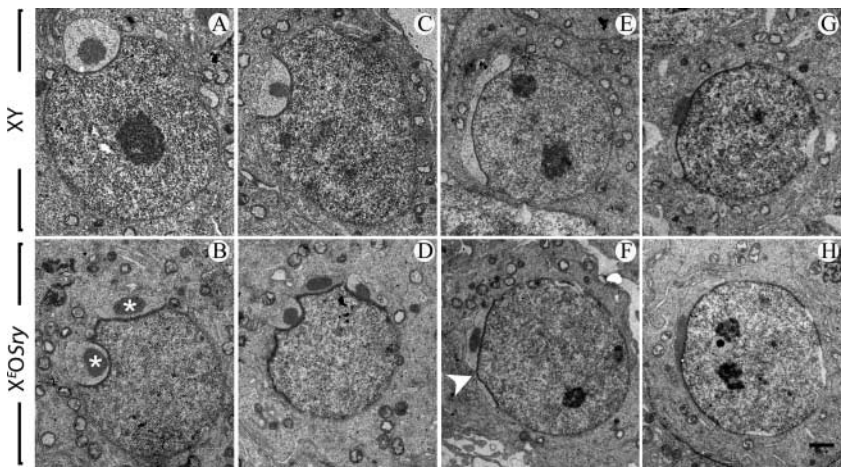

Figure 3 Aberrant acrosome development in XO male mice. Electron micrographs of round spermatids from XY control (A, C, E and G) and X^{E}O*Sry* (B, D, F and H) males. Different steps of maturation are represented. In the Golgi phase, step 3 spermatids show a normal acrosomal structure in XY (A) and a double acrosomal vesicle (each vesicle contains an acrosomal granule; stars) in X^{E}O*Sry* (B). At the beginning of the cap phase (C and D), the acrosome of step 4–5 spermatids flattens out on the nucleus and the acrosomal granule contacts the inner acrosomal membrane. While XY spermatids have a single acrosomal vesicle (C), double and here multiple acrosomal vesicles (D) are found in X^{E}O*Sry* spermatids. At the end of the cap phase (E and F), the acrosome has extended over one-third of the nuclear circumference in the XY (E). Double or here discontinuous acrosomes are found in step 6 spermatids of X^{E}O*Sry* male (F); arrowhead points to the acrosomal discontinuity. (G and H) In the acrosomal phase, acrosomes of X^{E}O*Sry* spermatids (H) were now indistinguishable from those of XY spermatids (G). Scale bar (in H): 1 μm (A, B, C and D), 1.25 μm (E, F, G and H).

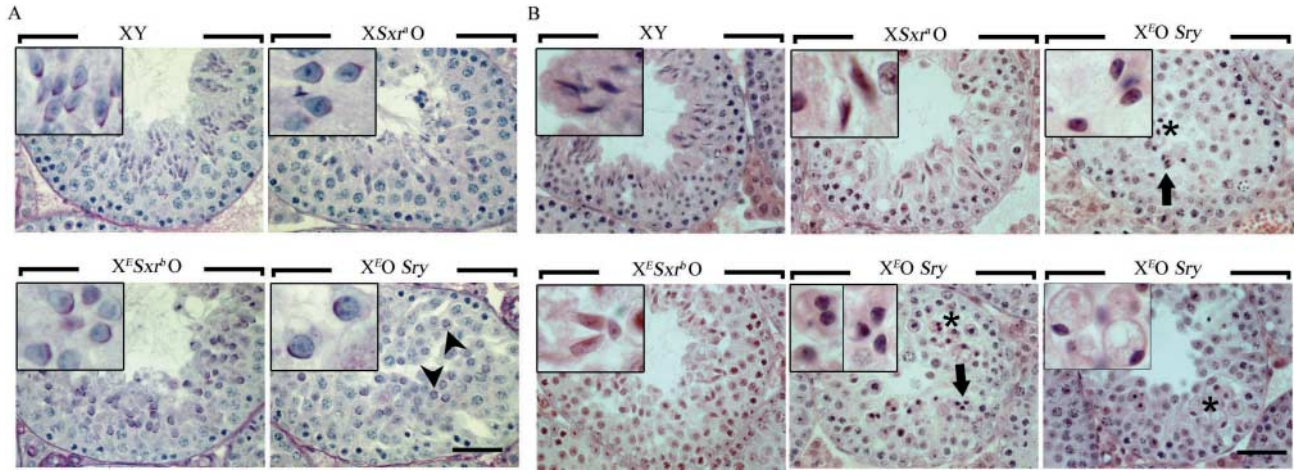

Figure 4 In X^{E}O*Sry* male mice, spermatids arrest and accumulate at round spermatid step 7 of their development whereas those of X^E*Sxr*^{b}O mice progress to elongating spermatid stages. Histological sections of testes from 6-week-old XY, X^{E}O*Sry*, X^E*Sxr*^{b}O and X*Sxr*^{a}O mice.
(A) PAS/haematoxylin-stained stage IX–X testis tubule sections. At this stage, elongation is clearly seen in XY and X*Sxr*^{a}O tubules but barely starts in X^E*Sxr*^{b}O tubules and is not seen in X^{E}O*Sry* (see corresponding inset). The round nuclear shape and the fact that the acrosome (purple staining) of X^{E}O*Sry* spermatids is often not facing towards the basal membrane (arrowheads) show that the spermatids are arrested at step 7 (they should be step 9–10). (B) H&E-stained stage XII-I testis tubule sections. We show stage XII-I seminiferous tubules because by that stage elongated spermatids should be properly formed. While in XY males, elongated spermatids form a hooked tip, this is lacking in X^E*Sxr*^{b}O and X*Sxr*^{a}O. By this stage, many of the arrested step 7 spermatids in X^{E}O*Sry* have been eliminated by shedding and apoptosis/necrosis. The few that remain have darkly stained nuclei (stars and corresponding insets), which very rarely may have an elongated shape (arrows and corresponding inset). However, similar elongated 'nuclei' are seen in large vesicular structures classically associated with apoptosis (bottom right panel). Scale bar, 40 μm. Insets represent a 3× magnification of some characteristic spermatids found in the corresponding pictures.

Sperm tail elongation is seen in spermatids of X^{E}Sxr^{b}O males but not in X^{E}OSry males

The development of the sperm tail is not easy to assess in testis sections. However, it occurs in conjunction with sperm head elongation in normal and X*Sxr*^{a}O males (Mahadevaiah *et al.* 1988), so it seemed likely that sperm tails would be formed in X^E*Sxr*^{b}O. To confirm this, we prepared silver-stained smears of testicular cell suspensions for all three XO male models (Fig. 6). Sperm with elongated tails were easily identified in the smears from X*Sxr*^{a}O males and, as might be expected, none were identified in smears from X^{E}O*Sry* males. In X^E*Sxr*^{b}O males, sperm with some tail development were also easily found, but the sperm tail elongation was generally less extensive than in X*Sxr*^{a}O males. Intriguingly, the sperm heads in X^E*Sxr*^{b}O males appeared less abnormal than those in X*Sxr*^{a}O males.

Discussion

In this study, we compared spermatid development in XO males with varying Yp gene complements: X^{E}O*Sry* (*Sry* and *Eif2s3y*), X^E*Sxr*^{b}O (*Rbmy1a1*, *H2al2y* (*Gm16501* and *Gm6026*), *Sry*, *Eif2s3y* and *Zfy2/1* fusion gene) and X*Sxr*^{a}O (*Rbmy1a1*, *H2al2y*, *Sry*, *Zfy2*, *Usp9y*, *Ddx3y*, *Uty*, *Eif2s3y*, *Kdm5d*, *Ube1y1* and *Zfy1*). As

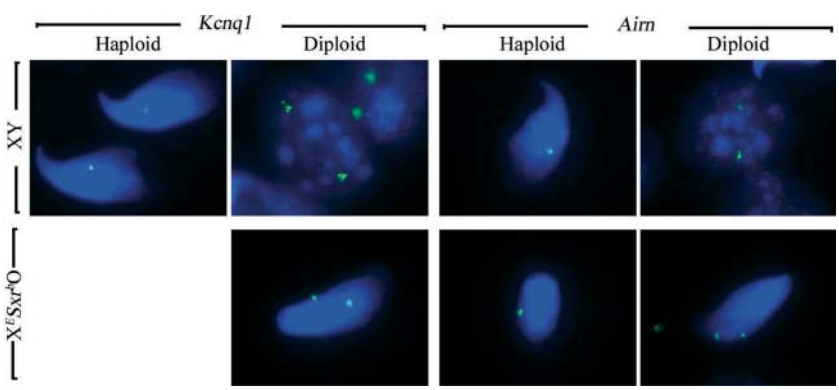

Figure 5 Both haploid and diploid spermatids from X^E*Sxr*^{b}O male mice are elongating. Spread cells from XY and X^E*Sxr*^{b}O testis stained by DNA FISH with autosomal probes for either *Kcnq1* or *Airn*. In XY males, for both probes, haploid elongated spermatids display a single DNA FISH spot whereas spermatogonia show two spots characteristic of diploid cells. In X^E*Sxr*^{b}O testis, haploid (one spot) and diploid (two spots) spermatids are elongating.

Table 3 The relative frequencies of haploid vs diploid spermatids at the round and elongating spermatid stages in 6-week-old XY and X^{E}*Sxr*^{b}O mice estimated by DNA FISH.

	Round spermatids			Elongated spermatids		
	Probe	Haploid[a]	Diploid[a]	Probe	Haploid[a]	Diploid[a]
XY	*Kcnq1*	50	0	*Kcnq1*	50	0
	Hist1h/Olfr1359	100	0	*Airn*	50	0
				Speer	50	0
	Total (%)	150 (100%)	0 (0%)	Total (%)	150 (100%)	0 (0%)
X^{E}*Sxr*^{b}O	*Kcnq1*	3	47	*Kcnq1*	0	50
	Airn	5	45	*Airn*	2	48
	Speer	2	97	*Speer*	7	43
	Total (%)	10 (5%)	189 (95%)	Total (%)	9 (6%)	141 (94%)

[a]Haploid and diploid spermatids were identified by DNA FISH as exemplified in Fig. 5 for the elongated spermatids.

previously reported for X*Sxr*^{a}O males, all three XO male genotypes produced diploid and haploid spermatids, as evidenced by ploidy analysis and acrosomal development, but the proportion of haploid spermatids was substantially lower in the two severely Yp-deficient genotypes. Acrosomal anomalies were observed in all three mouse models and were more frequent in diploid spermatids. Ploidy, *per se*, did not appear to affect the extent of spermiogenic progression, but Yp gene deficiency had clear effects with delayed sperm head and tail morphogenesis in X*Sxr*^{b}O males and a lack of sperm head elongation and extension of the axoneme to form the sperm tail in X^{E}O*Sry* males. The results are summarised in Fig. 7.

Achievement of the second meiotic division in XO males

Our data show that haploid and diploid spermatids are present in all three XO male genotypes with the proportion of haploid increasing between 30 days and 6 weeks of age, but the proportion of haploid spermatids is markedly higher in X*Sxr*^{a}O males than in the two Yp gene-deficient genotypes. Drawing any conclusion as to the cause of this latter difference is complicated by the fact that X*Sxr*^{a}O males have a robust, *Zfy2*-dependent, apoptotic elimination of spermatocytes at MI, which reduces spermatid counts to ~3% of XY controls, while both types of Yp-deficient XO males have a severely attenuated response because they lack the Y-encoded gene *Zfy2* (Sutcliffe *et al.* 1991, Vernet *et al.* 2011). The *Zfy2*-dependent apoptotic response is considered to be a consequence of the univalent X chromosome triggering an MI spindle assembly checkpoint (MI SAC; Burgoyne *et al.* 1992, Vernet *et al.* 2011). We must therefore first consider how this difference in apoptotic response may impact on haploid vs diploid spermatid frequencies.

The existence of an MI SAC in mammals has been well documented from studies of mouse oocytes (reviewed by Sun & Kim (2012)). In the present context, the XO female mouse is most relevant for comparison with the Yp gene-deficient mouse models because in female meiosis triggering the MI SAC does not elicit an apoptotic response. XO oocytes complete both meiotic divisions, despite the fact that the X has no pairing partner and thus is predisposed to trigger the MI SAC (LeMaire-Adkins *et al.* 1997). The failure to trigger MI arrest is explained by recent data showing that the first meiotic division in oocytes can proceed once a 'critical mass' of kinetochores have achieved correct attachment to the spindle (Hoffmann *et al.* 2011, Nagaoka *et al.* 2011) – a univalent X with 1 or 2 unattached kinetochores is therefore insufficient to maintain MI arrest. In the light of the findings in XO females, it might therefore be

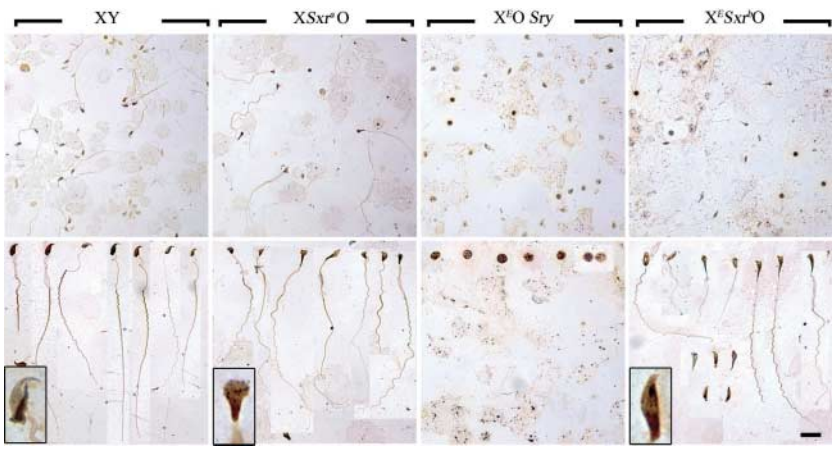

Figure 6 Sperm tail development is observed in X^{E}*Sxr*^{b}O male mice. Silver-stained sperm smears from 6-week-old XY, X*Sxr*^{a}O, X^{E}O*Sry* and X^{E}*Sxr*^{b}O mouse testes. The top panel is a low magnification of the smear, showing the relative density of the cells found in each specimen. The bottom panel is a montage of the elongated spermatids/sperm found in each sample. Note that no elongated spermatids could be found in the X^{E}O*Sry* sample and what we believe to be the arrested round spermatids are presented instead. An example of the most characteristic sperm head for each genotype is represented at a higher magnification in the inset of the bottom panels. Scale bar: 32.5 μm (top panel), 20 μm (bottom panel).

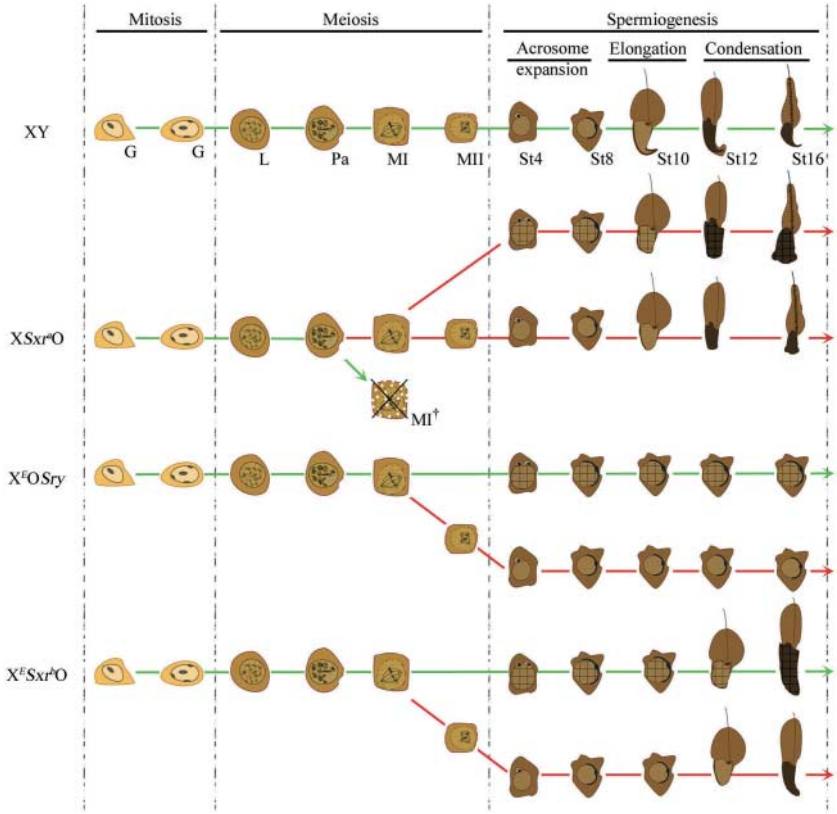

Figure 7 Schematic representation of spermatogenesis events occurring in XY, X*Sxr*^{a}O, X^{E}O*Sry* and X^E*Sxr*^{b}O male mice. The green lines represent the main pathway followed by the germ cells. Three phases are represented: mitosis, meiosis and spermiogenesis. No difference in the mitotic phase could be observed between the genotypes represented; however, differences start to be seen at the end of the first meiotic division. Previously published work has shown that major apoptotic elimination occurs at MI in X*Sxr*^{a}O mice (MI† crossed out cell) but not in X^{E}O*Sry* or X^E*Sxr*^{b}O mice. The germ cells that evade apoptotic elimination in X*Sxr*^{a}O progress in an equal proportion to spermiogenesis events with or without completion of the second meiotic division resulting in a mix of haploid and diploid spermatids (cross ruled cells). Most of the germ cells in X^{E}O*Sry* or X*Sxr*^{b}O mice do not achieve the second meiotic division resulting in a majority of diploid spermatids. Anomalies in the early phases of acrosomal development could be observed, particularly for the diploid spermatids, of X*Sxr*^{a}O, X^{E}O*Sry* and X^E*Sxr*^{b}O males (represented by double acrosomal structure at the nucleus of diploid spermatids). However, later phases of acrosomal development were normal for diploid as for haploid spermatids. The timing of the elongation and condensation phases of spermiogenesis is normal in X*Sxr*^{a}O mice, while no elongation/condensation could be observed in X^{E}O*Sry*. Sperm head elongation and condensations are achieved in X^E*Sxr*^{b}O but both these steps are delayed. Sperm tail develops as the sperm head elongates. Note that the most mature spermatids obtained in X*Sxr*^{a}O males have a mushroom-shaped head while the heads of X^E*Sxr*^{b}O spermatids have a somewhat more normal shape. G, spermatogonia; L, leptotene spermatocyte; Pa, pachytene spermatocyte; MI, metaphase of the meiosis I; MII, metaphase of the meiosis II; St4–16, spermatids from steps 4 to 16.

expected that XO spermatocytes in the Yp-deficient models (which lack an apoptotic response) would complete both meiotic divisions to become haploid spermatids, but in fact, we have found the majority of spermatids are diploid (at 6 weeks X^{E}O*Sry* had 88.6% and X^E*Sxr*^{b}O 94.8% diploid spermatids). As we have shown, X*Sxr*^{a}O males have a substantially lower proportion of diploid spermatids (55.9% at 6 weeks); this could be explained if MI spermatocyte apoptosis preferentially removes those that are destined to form diploid spermatids, but the more exciting possibility is that a Yp gene or genes retained in *Sxr*^{a} promotes the second meiotic division.

In XO females, it has been shown that in a proportion of oocytes, the X univalent achieves bipolar attachment to the spindle followed by segregation of the two sister chromatids; however, this is not a prerequisite for completion of the first meiotic division (Hunt *et al.* 1995, Hodges *et al.* 2001). This phenomenon has not been documented in males, but this is probably because the apoptotic response in X*Sxr*^{a}O males is so efficient that there are almost no anaphase plates available for study. We have therefore started to look for evidence of bipolar attachment and segregation in X^{E}O*Sry* males. Our preliminary data suggest that bipolar attachment and segregation do take place, but it seems the more common fate is that the X univalent fails to attach to the spindle and is left stranded in a micronucleus (see Supplementary Table 1 and Supplementary Materials and Methods, see section on supplementary data given at the end of this article).

What is the explanation for the dramatic difference between XO females and the Yp gene-deficient XO males, with respect to completion of the second meiotic

division? One striking difference between the meiotic divisions of females and males is that in females the chromosomes remain condensed throughout both meiotic divisions, whereas in males there is a transcriptionally active 'interphasic secondary spermatocyte' stage between the two meiotic divisions (Monesi 1964, Kudo *et al*. 2009, Vernet *et al*. 2011). This begs the question as to why meiosis in males requires this brief interphase between the two meiotic divisions, while meiosis in females does not. Our hypothesis is that this is to allow expression of X and/or Y genes with important functions during the divisions, but which in males (but not females) are silenced throughout pachytene and diplotene as a consequence of meiotic sex chromosome inactivation (reviewed by Turner (2007)). This model would allow for there being some Yp gene activity during this interphase that facilitates the re-condensation of the chromosomes and progression through the second division. In order to investigate this possibility, we need to compare males with the three different Yp gene complements used here but without the major difference in apoptotic selection. The apoptotic elimination in X*Sxr*^{a}O males can be prevented by adding a minute PAR-bearing chromosome that enables the formation of a minimal sex bivalent; this restores round spermatid counts to normal (Sutcliffe *et al*. 1991, Burgoyne *et al*. 1992) with 96% haploid spermatids (N Vernet & P S Burgoyne, unpublished observations). We are therefore introducing this chromosome into all three genotypes in order to compare the extent to which the three Yp gene complements enable completion of the second meiotic division.

Acrosome anomalies in XO males

Our present studies indicate that in all three XO mouse models, the haploid and diploid products of meiosis enter spermiogenesis and that the initiation of acrosome development is not delayed. This shows that a Yp gene complement of just *Sry* and *Eif2s3y* is sufficient to support this initial phase of spermiogenesis. However, in all three XO male models, at the onset of the cap phase of acrosome development, we observed a high incidence of spermatids that had two or more acrosomal structures, instead of the normal single acrosomal structure. Morphologically abnormal spermatids with a deposition of 'multiple pro-acrosomal granules' were previously described in X*Sxr*^{a}O mice (Kot & Handel 1990). In our more detailed analysis of all three XO male mouse models, we found frequent abnormal acrosome development in diploid spermatids resulting in multiple acrosomal structures during the cap phase. This fragmented acrosome was no longer apparent by the end of the cap phase. Our TEM analysis of X^{E}O*Sry* males shows intact acrosomal granules and suggests that there is fusion of the multiple acrosomal vesicles and granules after they become closely apposed to the nucleus. Although it is clear that diploid spermatids have an elevated incidence of multiple acrosome structures during the cap phase in XO males (53–63% in X*Sxr*^{a}O males), we nevertheless found 9–16% in haploid spermatids from X*Sxr*^{a}O males and a similar frequency in (haploid) spermatids from XY males. Descriptions of acrosome development in the mouse (Oakberg 1956*a*, Russell *et al*. 1990) describe the clustering of Golgi vesicles containing proacrosomic granules to form a large vesicle containing a single acrosomic granule; this associates with the nuclear envelope to mark the beginning of the 'cap phase', which covers spermatid stages 4–5 (in tubule stages IV–V). Nevertheless, the acrosomal cap continues to enlarge by the fusion of further Golgi vesicles and the fact that we are seeing some 'multiple acrosome structures' in Lectin–PNA-stained sections of stage IV–V tubules from XY control males (and in haploid spermatids from XO males) may be due to classification of some of the ongoing fusions as multiple acrosomal structures.

Evidence of Y gene functions in sperm head remodelling and sperm tail elongation

Our current findings show that in X^{E}OSry males, there is an almost total block at step 7 of round spermatid development, with the result that elongation and restructuring of the nucleus to form the sperm head, and extension of the axoneme to form the sperm tail, does not take place. Intriguingly, a block at the start of spermatid elongation is also seen in mice carrying a *Brca1* gene from which the E3 ligase activity was deleted (Shakya *et al*. 2011) and in *Dicer1* knockout mice (Korhonen *et al*. 2011). Because sperm head remodelling and sperm tail elongation are achieved in both X*Sxr*^{a}O (Mahadevaiah *et al*. 1988, Kot & Handel 1990) and X^E*Sxr*^{b}O (albeit delayed), we conclude that these processes require genetic information present in *Sxr*^{a} that is at least partially retained in *Sxr*^{b}. The protein coding genes that *Sxr*^{a} and *Sxr*^{b} have in common are *Sry*, an estimated seven copies of *Rbmy1a1* (Mahadevaiah *et al*. 1998) and two copies of *H2al2y (Gm16501* and *Gm6026)*; *Sxr*^{b} also includes a transcribed *Zfy2/1* fusion gene while *Sxr*^{a} has retained the single copies of *Zfy1* and *Zfy2* from which the fusion gene was derived by an ectopic recombination event (Simpson & Page 1991). *Rbmy1a1* is unlikely to be involved in spermiogenesis as it is transcribed only in spermatogonia and early spermatocytes, and no RBMY protein has been detected in spermatids (Szot *et al*. 2003, Lee *et al*. 2004). *H2al2y*, which encodes a variant H2A histone, is a strong candidate for sperm head restructuring as it is not detected at 21 dpp but starts to be transcribed from 23 dpp onwards; an age at which the transition from round to elongated spermatids takes place (Ferguson *et al*. 2009). To test this possibility, we have reinstated *H2al2y* expression in X^{E}O*Sry* males by adding a

transgenic copy of *H2al2y* driven by the spermatid-specific mouse protamine-1 promoter. Disappointingly, this failed to enable sperm head elongation (or sperm tail formation) (Supplementary Figure 3 and Supplementary Materials and Methods, see section on supplementary data given at the end of this article).

The *Zfy2/1* fusion gene is also an attractive candidate for the Yp spermiogenic function that is at least partially retained in Sxr^b. *Zfy1* and *Zfy2* encode putative transcription factors and *Zfy2* in particular is likely to be important for spermiogenesis because it has acquired an additional *Cypt*-derived promoter that drives strong expression in spermatids (Hansen *et al*. 2006). The *Zfy2/1* fusion gene is also strongly expressed in spermatids because the promoter elements are derived from *Zfy2*; however, the transcripts produced are spliced like those of *Zfy1* so that a substantial proportion of the transcripts will lack the exon 6 encoding the transcriptional activation domain required for transcription factor function (Decarpentrie *et al*. 2012). Thus, it is reasonable to suppose that both could promote sperm morphogenesis but the fusion gene would be less effective. In principle, this might be tested by comparing the separate addition of *Zfy2* and *Zfy2/1* transgenes to $X^E O Sry$ males. However, we already know that adding *Zfy2* reinstates the apoptotic elimination of MI spermatocytes with a univalent X chromosome whereas the addition of Sxr^b (that includes the *Zfy2/1* fusion gene) does not (Vernet *et al*. 2011). We are therefore carrying out these transgene additions in conjunction with the introduction of the minute PAR-bearing chromosome mentioned earlier, in order to avoid triggering this apoptotic response (Burgoyne *et al*. 1992).

One surprising observation was that the developing sperm head seen in cell spreads from $X^E Sxr^b O$ testes looked healthier and better hooked than those from $XSxr^a O$ testes. The same observation was independently made by collaborators using testicular 'sperm' from $X^E Sxr^b O$ males for ICSI (Monika Ward and Yasuhiro Yamauchi, personal communication). In considering why this might be, it is important to take account of the fact that in XY males there is substantial repression of X and Y gene expression in spermatids (Namekawa *et al*. 2006, Turner *et al*. 2006). This repression is promoted by the activity of the multiple copy Y gene *Sly* that is present on the Y long-arm and encodes a protein that localises to the X and Y chromatin domains of round spermatids (Cocquet *et al*. 2009). In XO males, the lack of the long arm inevitably leads to a de-repression of spermatid-expressed X and Y genes, and it is this de-repression that is undoubtedly responsible for the sperm head abnormalities that are a feature of mice with Y long-arm deficiencies (Ellis *et al*. 2005, Cocquet *et al*. 2009). One possibility is that a Y-linked gene present in Sxr^a but not in Sxr^b, and that is up-regulated in the Y long-arm deficient mice, causes the more severely aberrant sperm head development observed in $XSxr^a O$ mice.

In conclusion, our findings show that spermiogenesis is initiated in XO male mice whether or not the second meiotic division has taken place, and even when the only Y genes present are *Sry* and *Eif2s3y*. However, genetic information from Yp that is present in Sxr^a is necessary for initiation of the sperm morphogenesis that characterises the elongation phase of spermatid development and perhaps also for the efficient completion of the second meiotic division.

Materials and Methods

Animals

All mice in this study have a random-bred MF1 (NIMR colony) background. To produce the XO males, we mated $X^{Paf}O$ females (carrying the X-linked *Patchy-fur* mutation as a coat marker; Lane & Davisson 1990) to i) '$X^E Y Sxr^b$' males that have the X-linked *Eif2s3y* transgene (Mazeyrat *et al*. 2001) and a Y chromosome that has the $Tp(Y)1Ct^{Sxr\text{-}b}$ sex reversal factor (Simpson & Page 1991, Mazeyrat *et al*. 1998) attached distal to its pseudoautosomal region, this cross produces $X^E Sxr^b O$ males with a normal coat; ii) '$X^E Y^{\Delta Sry} Sry$' males that have the X carrying the *Eif2s3y* transgene (Mazeyrat *et al*. 2001), a Y chromosome with an 11 kb deletion removing *Sry* (*dl1Rlb*) (Gubbay *et al*. 1990, 1992) and an autosomally located *Sry* transgene (Tg(Sry)2Ei) (Mahadevaiah *et al*. 1998), this cross produces $X^E O Sry$ males with a normal coat; and iii) '$XY Sxr^a$' males that have a Y chromosome that has the $Tp(Y)1Ct^{Sxr\text{-}a}$ sex reversal factor (Cattanach *et al*. 1971) attached distal to its pseudoautosomal region, this cross produces $XSxr^a O$ males with a normal coat. MF1 XY^{RIII} males were used as normal controls; Y^{RIII} is the strain of Y chromosome from which Sxr^b and Sxr^a derive. All animal procedures were in accordance with the United Kingdom Animal Scientific Procedures Act 1986 and were subject to local ethical review.

Ploidy analysis on testis cell spreads

Nuclear DNA content was measured on surface-spread spermatogenic cells from 30 dpp and 6-week-old testes as described previously (Vernet *et al*. 2011) using synaptonemal complex SYCP3 staining and DAPI fluorescence intensity measurements. The cells quantified were pachytene spermatocytes (4C), spermatogonia (2C) and spermatids (2C or 1C) distinguished from secondary spermatocytes based on the SYCP3 staining pattern (Kudo *et al*. 2009, Vernet *et al*. 2011). While secondary spermatocyte interphase nuclei and early diploid spermatids contain around ten chromocentra, later diploid spermatids and haploid spermatids show three to five DAPI bright chromocentra and one chromocentrum respectively. After integrated intensity measurement of DAPI fluorescence, the values were adjusted to give an arbitrary value of 4 for pachytene spermatocyte nuclei and the measurement obtained for the nuclei of the other cell types was normalised to the value of the nearest pachytene spermatocyte found on the slide. Spermatids were considered as diploid if the value obtained was above the lowest value obtained for the spermatogonia. The other spermatids

were considered to be haploid. Percentage of haploid spermatids was calculated after measurement of 50–100 spermatids for each of the three to four males analysed per genotype at each age. ANOVA analysis (General linear models, NCSS, Kaysville, UT, USA) was carried out after angular transformation of percentages.

Histological analysis

For standard histological analysis, testes were fixed in Bouin, rinsed with 70% ethanol, embedded in paraffin wax, sectioned at 5 μm on glass slides, and stained with H&E. Stages of seminiferous tubules were identified by the composition of germ cells near the basal membrane, as described in Ahmed & de Rooij (2009).

Acrosome formation was monitored on testis sections by i) PAS staining (which highlights the developing acrosome) of paraffin wax sections from Bouin-fixed testis followed by haematoxylin counterstaining and ii) fluorescence-tagged Lectin–PNA staining of the outer acrosomal membrane using paraformaldehyde (PFA)-fixed wax sections. For the latter, testes were fixed in 4% PFA diluted in PBS overnight at 4 °C and rinsed with 70% ethanol before embedding in paraffin wax. Sections (5 μm) on a glass slide were de-waxed, processed for antigen retrieval, washed in PBS and blocked for 30 min at room temperature in PBST–BSA (PBS containing 0.1% Tween 20 and 0.15% BSA). Immunolabelling for the synaptonemal complex protein SYCP3 (used as a stage marker) was performed with rabbit polyclonal anti-SYCP3 (1:100; Abcam, Cambridge, UK) diluted in PBST–BSA incubated overnight at 37 °C. Slides were then washed in PBST, incubated at 37 °C for 1 h with a mix of chicken anti-rabbit Alexa 488 (1:500; Molecular Probes, Paisley, UK) and Alexa Fluor 594-conjugated Lectin–PNA (1:700; Invitrogen Life Technologies) diluted in PBS and then washed in PBST before mounting in a medium containing DAPI (Vectashield with DAPI; Vector Laboratories, Burlingame, CA, USA). Seminiferous epithelium stages were judged from the DAPI staining and the expression pattern of SYCP3 that remains at the sister chromatids until diploid and haploid spermatids reach epithelial stages II–III (Vernet *et al.* 2011).

For the quantitation of acrosomal defects, we analysed spermatids from stage IV–V seminiferous tubules from two 6-week-old X*Sxr*^{a}O males. Haploid and diploid spermatids were discriminated based on nuclear size, DAPI morphology and the SYCP3 staining pattern.

Transmission electron microscopy

Mice were perfused, through the left ventricle (Vernet *et al.* 2006), with ice-cold 2.5% glutaraldehyde fixative diluted in PBS. The testes were dissected, left for 1 h in the fixative, and cut into small blocks that were kept at 4 °C in the same fixative until embedding. Testes were post-fixed for 1 h in 1% osmium tetroxide, stained 'en bloc' for 1 h with 1% aqueous uranyl acetate, dehydrated with graded alcohol series and embedded in Epon. Ultrathin sections (60 nm) were contrasted 7 min with uranyl acetate and lead citrate and then examined using JEOL 1200EX electron microscope.

DNA fluorescence in situ *hybridization*

Fluorescence *in situ* hybridization (FISH) was performed on surface-spread spermatogenic cells from adult testes, as described previously (Turner *et al.* 2006). Digoxigenin-labelled probes were prepared using the Digoxigenin Nick Translation Kit (Roche Diagnostics), and hybridisations were carried out. The probes used against autosomal loci were chromosome 7 BAC RP23-101N20 containing one copy of the *Kcnq1* locus, the chromosome 17 BAC RP23-432O2 containing one copy of the *Airn* locus, the chromosome 13 BAC RP23-423B15 containing several members of *Hist1h* family and *Olfr1359* locus and the chromosome 5 BAC RP23-212A20 containing one copy of the *Speer* locus (BACPAC Resources Center, Children's Hospital Oakland Research Institute, Oakland, CA, UK). After stringency washes, DNA FISH signals were developed using anti-DIG-FITC (Chemicon, Temecula, CA, USA) diluted 1:10 for 1 h at 37 °C. Staging of spermatogenic cells was based on DAPI fluorescence morphology, together with immunolabelling for SYCP3 (1/100; Abcam) and the phosphorylated histone H2AFX (γH2AX) detected by a mouse MAB (1/300; Upstate, Hampshire, UK), as described previously (Turner *et al.* 2005).

Supplementary data

This is linked to the online version of the paper at http://dx.doi.org/10.1530/REP-12-0158.

Declaration of interest

The authors declare that there is no conflict of interest that could be perceived as prejudicing the impartiality of the research reported.

Funding

The work was funded by the Medical Research Council UK (P S Burgoyne: U117532009, N Vernet: MRC CDF) and EMBO (N Vernet).

Acknowledgements

The authors thank Ms Aine Rattigan and Mr Obah A Ojarikre for assistance with genotype analyses and mouse colony management respectively, as well as Ms Liz Hirst and Dr Radma Mahmood for kind assistance with electron microscopy and histological analyses respectively. NIMR Procedural Services generated the transgenics and Biological services provided help with mouse breeding.

References

Ahmed EA & de Rooij DG 2009 Staging of mouse seminiferous tubule cross-sections. *Methods in Molecular Biology* **558** 263–277.

de Boer P, Searle AG, van der Hoeven FA, de Rooij DG & Beechey CV 1986 Male pachytene pairing in single and double translocation heterozygotes and spermatogenic impairment in the mouse. *Chromosoma* **93** 326–336. (doi:10.1007/BF00327591)

Burgoyne PS, Mahadevaiah SK, Sutcliffe MJ & Palmer SJ 1992 Fertility in mice requires X-Y pairing and a Y-chromosomal "spermiogenesis" gene mapping to the long arm. *Cell* **71** 391–398. (doi:10.1016/0092-8674(92)90509-B)

Cattanach BM, Pollard CE & Hawkes SG 1971 Sex reversed mice: XX and XO males. *Cytogenetics* **10** 318–337. (doi:10.1159/000130151)

Cocquet J, Ellis PJ, Yamauchi Y, Mahadevaiah SK, Affara NA, Ward MA & Burgoyne PS 2009 The multicopy gene Sly represses the sex chromosomes in the male mouse germline after meiosis. *PLoS Biology* **7** e1000244. (doi:10.1371/journal.pbio.1000244)

Decarpentrie F, Vernet N, Mahadevaiah SK, Longepied G, Streichemberger E, Aknin-Seifer I, Ojarikre OA, Burgoyne PS, Metzler-Guillemain C & Mitchell MJ 2012 Human and mouse ZFY genes produce a conserved testis-specific transcript encoding a zinc finger protein with a short acidic domain and modified transactivation potential. *Human Molecular Genetics* **21** 2631–2645. (doi:10.1093/hmg/dds088)

Ellis PJI, Clemente EJ, Ball P, Toure A, Ferguson L, Turner JMA, Loveland KL, Affara NA & Burgoyne PS 2005 Deletions on mouse Yq lead to upregulation of multiple X- and Y-linked transcripts in spermatids. *Human Molecular Genetics* **14** 2705–2715. (doi:10.1093/hmg/ddi304)

Ferguson L, Ellis PJ & Affara NA 2009 Two novel mouse genes mapped to chromosome Yp are expressed specifically in spermatids. *Mammalian Genome* **20** 193–206. (doi:10.1007/s00335-009-9175-8)

Gubbay J, Collignon J, Koopman P, Capel B, Economou A, Munsterberg A, Vivian N, Goodfellow P & Lovell-Badge R 1990 A gene mapping to the sex-determining region of the mouse Y chromosome is a member of a novel family of embryonically expressed genes. *Nature* **346** 245–250. (doi:10.1038/346245a0)

Gubbay J, Vivian N, Economou A, Jackson D, Goodfellow P & Lovell-Badge R 1992 Inverted repeat structure of the Sry locus in mice. *PNAS* **89** 7953–7957. (doi:10.1073/pnas.89.17.7953)

Hannappel E & Drews U 1979 Mosaic character of spermatogenesis in carriers of the "sex reversed" factor in the mouse. *Hormone and Metabolic Research* **11** 682–689. (doi:10.1055/s-0028-1092800)

Hannappel E, Siegler W & Drews U 1980 Demonstration of 2n spermatids in carriers of the "Sex Reversed" factor in the mouse by Feulgen cytophotometry. *Histochemistry* **69** 299–306. (doi:10.1007/BF00489775)

Hansen MA, Nielsen JE, Tanaka M, Almstrup K, Skakkebaek NE & Leffers H 2006 Identification and expression profiling of 10 novel spermatid expressed CYPT genes. *Molecular Reproduction and Development* **73** 568–579. (doi:10.1002/mrd.20463)

Hodges CA, LeMaire-Adkins R & Hunt PA 2001 Coordinating the segregation of sister chromatids during the first meiotic division: evidence for sexual dimorphism. *Journal of Cell Science* **114** 2417–2426.

Hoffmann S, Maro B, Kubiak JZ & Polanski Z 2011 A single bivalent efficiently inhibits cyclin B1 degradation and polar body extrusion in mouse oocytes indicating robust SAC during female meiosis I. *PLoS ONE* **6** e27143. (doi:10.1371/journal.pone.0027143)

Hunt P, LeMaire R, Embury P, Sheean L & Mroz K 1995 Analysis of chromosome behaviour in intact mammalian oocytes:monitoring the segregation of a univalent chromosome during female meiosis. *Human Molecular Genetics* **4** 2007–2012. (doi:10.1093/hmg/4.11.2007)

Korhonen HM, Meikar O, Yadav RP, Papaioannou MD, Romero Y, Da Ros M, Herrera PL, Toppari J, Nef S & Kotaja N 2011 Dicer is required for haploid male germ cell differentiation in mice. *PLoS ONE* **6** e24821. (doi:10.1371/journal.pone.0024821)

Kot MC & Handel MA 1990 Spermatogenesis in XO,Sxr mice: role of the Y chromosome. *Journal of Experimental Zoology* **256** 92–105. (doi:10.1002/jez.1402560112)

Kudo NR, Anger M, Peters AH, Stemmann O, Theussl HC, Helmhart W, Kudo H, Heyting C & Nasmyth K 2009 Role of cleavage by separase of the Rec8 kleisin subunit of cohesin during mammalian meiosis I. *Journal of Cell Science* **122** 2686–2698. (doi:10.1242/jcs.035287)

Lane PW & Davisson MT 1990 Patchy fur (*Paf*), a semidominant X-linked gene associated with a high level of X-Y nondisjunction in male mice. *Journal of Heredity* **81** 43–50.

Lee J, Hong J, Kim E, Kim K, Kim SW, Krishnamurthy H, Chung SS, Wolgemuth DJ & Rhee K 2004 Developmental stage-specific expression of Rbm suggests its involvement in early phases of spermatogenesis. *Molecular Human Reproduction* **10** 259–264. (doi:10.1093/molehr/gah037)

LeMaire-Adkins R, Radke K & Hunt PA 1997 Lack of checkpoint control at the metaphase/anaphase transition: a mechanism of meiotic nondisjunction in mammalian females. *Journal of Cell Biology* **139** 1611–1619. (doi:10.1083/jcb.139.7.1611)

Levy ER & Burgoyne PS 1986 Diploid spermatids: a manifestation of spermatogenic impairment in XOSxr and T31H/+ male mice. *Cytogenetics and Cell Genetics* **42** 159–163. (doi:10.1159/000132269)

Mahadevaiah SK, Setterfield LA & Mittwoch U 1988 Univalent sex chromosomes in spermatocytes of Sxr-carrying mice. *Chromosoma* **97** 145–153. (doi:10.1007/BF00327371)

Mahadevaiah SK, Odorisio T, Elliott DJ, Rattigan A, Szot M, Laval SH, Washburn LL, McCarrey JR, Cattanach BM, Lovell-Badge R *et al.* 1998 Mouse homologues of the human AZF candidate gene RBM are expressed in spermatogonia and spermatids, and map to a Y chromosome deletion interval associated with a high incidence of sperm abnormalities. *Human Molecular Genetics* **7** 715–727. (doi:10.1093/hmg/7.4.715)

Mazeyrat S, Saut N, Sargent CA, Grimmond S, Longepied G, Ehrmann IE, Ellis PS, Greenfield A, Affara NA & Mitchell MJ 1998 The mouse Y chromosome interval necessary for spermatogonial proliferation is gene dense with syntenic homology to the human AZFa region. *Human Molecular Genetics* **7** 1713–1724. (doi:10.1093/hmg/7.11.1713)

Mazeyrat S, Saut N, Grigoriev V, Mahadevaiah SK, Ojarikre OA, Rattigan A, Bishop C, Eicher EM, Mitchell MJ & Burgoyne PS 2001 A Y-encoded subunit of the translation initiation factor Eif2 is essential for mouse spermatogenesis. *Nature Genetics* **29** 49–53. (doi:10.1038/ng717)

Monesi V 1964 Ribonucleic acid synthesis during mitosis and meiosis in the mouse testis. *Journal of Cell Biology* **22** 521–532. (doi:10.1083/jcb.22.3.521)

Mori C, Allen JW, Dix DJ, Nakamura N, Fujioka M, Toshimori K & Eddy EM 1999 Completion of meiosis is not always required for acrosome formation in HSP70-2 null mice. *Biology of Reproduction* **61** 813–822. (doi:10.1095/biolreprod61.3.813)

Nagaoka SI, Hodges CA, Albertini DF & Hunt PA 2011 Oocyte-specific differences in cell-cycle control create an innate susceptibility to meiotic errors. *Current Biology* **21** 651–657. (doi:10.1016/j.cub.2011.03.003)

Namekawa SH, Park PJ, Zhang LF, Shima JE, McCarrey JR, Griswold MD & Lee JT 2006 Postmeiotic sex chromatin in the male germline of mice. *Current Biology* **16** 660–667. (doi:10.1016/j.cub.2006.01.066)

Oakberg EF 1956*a* A description of spermiogenesis in the mouse and its use in analysis of the cycle of the seminiferous epithelium and germ cell renewal. *American Journal of Anatomy* **99** 391–413. (doi:10.1002/aja.1000990303)

Oakberg EF 1956*b* Duration of spermatogenesis in the mouse and timing of stages of the cycle of the seminiferous epithelium. *American Journal of Anatomy* **99** 507–516. (doi:10.1002/aja.1000990307)

Russell LD, Ettlin RA, Sinha-Hikim AP & Clegg ED 1990 Histological and histopathological evaluation of the testis. 1st edn. Vienna, IL, USA: Cache River Press.

Shakya R, Reid LJ, Reczek CR, Cole F, Egli D, Lin CS, deRooij DG, Hirsch S, Ravi K, Hicks JB *et al.* 2011 BRCA1 tumor suppression depends on BRCT phosphoprotein binding, but not its E3 ligase activity. *Science* **334** 525–528. (doi:10.1126/science.1209909)

Simpson EM & Page DC 1991 An interstitial deletion in mouse Y chromosomal DNA created a transcribed Zfy fusion gene. *Genomics* **11** 601–608. (doi:10.1016/0888-7543(91)90067-O)

Sun SC & Kim NH 2012 Spindle assembly checkpoint and its regulators in meiosis. *Human Reproduction Update* **18** 60–72. (doi:10.1093/humupd/dmr044)

Sutcliffe MJ, Darling SM & Burgoyne PS 1991 Spermatogenesis in XY, XYSxra and XOSxra mice: a quantitative analysis of spermatogenesis throughout puberty. *Molecular Reproduction and Development* **30** 81–89. (doi:10.1002/mrd.1080300202)

Szot M, Grigoriev V, Mahadevaiah SK, Ojarikre OA, Tour A, Von Glasenapp E, Rattigan A, Turner JM, Elliott DJ & Burgoyne PS 2003 Does Rbmy have a role in sperm development in mice? *Cytogenetic and Genome Research* **103** 330–336. (doi:10.1159/000076821)

Turner JM 2007 Meiotic sex chromosome inactivation. *Development* **134** 1823–1831. (doi:10.1242/dev.000018)

Turner JM, Mahadevaiah SK, Fernandez-Capetillo O, Nussenzweig A, Xu X, Deng CX & Burgoyne PS 2005 Silencing of unsynapsed meiotic chromosomes in the mouse. *Nature Genetics* **37** 41–47. (doi:10.1038/ng1484)

Turner JM, Mahadevaiah SK, Ellis PJ, Mitchell MJ & Burgoyne PS 2006 Pachytene asynapsis drives meiotic sex chromosome inactivation and leads to substantial postmeiotic repression in spermatids. *Developmental Cell* **10** 521–529. (doi:10.1016/j.devcel.2006.02.009)

Vernet N, Dennefeld C, Rochette-Egly C, Oulad-Abdelghani M, Chambon P, Ghyselinck NB & Mark M 2006 Retinoic acid metabolism and signaling pathways in the adult and developing mouse testis. *Endocrinology* **147** 96–110. (doi:10.1210/en.2005-0953)

Vernet N, Mahadevaiah SK, Ojarikre OA, Longepied G, Prosser HM, Bradley A, Mitchell MJ & Burgoyne PS 2011 The Y-encoded gene *Zfy2* acts to remove cells with unpaired chromosomes at the first meiotic metaphase in male mice. *Current Biology* **21** 787–793. (doi:10.1016/j.cub.2011.03.057)

Received 27 April 2012
First decision 30 May 2012
Revised manuscript received 29 June 2012
Accepted 2 August 2012